DOE/ER/04831--T2

DOE/ER/04831--T2

DE83 017438

WEAK DECAYS AND DOUBLE BETA DECAY

Annual Progress Report
for Period January 1, 1983 - December 31, 1983

H.W. Nicholson

Mount Holyoke College

South Hadley, Massachusetts 01075

August 1983

Prepared for

The U.S. Department of Energy under Contract No. DE-AC02-78ER04831

DISCLAIMER

ABSTRACT

Work to measure the Σ^+ 0 degree differential cross section in the reaction $K^-p \rightarrow \Sigma^+\pi^-$ at several incident K^- momenta between 600 and 800 MeV/c as well as the asymmetries in the decays of polarized Σ^+'s into protons and neutral pions and of polarized Σ^-'s into neutrons and negative pions in collaboration with experimenters from Yale, Brookhaven, and the University of Pittsburgh (Brookhaven experiment 702) has been completed. Data from this experiment is currently being analyzed at Yale.

Work is currently underway to develop and construct an experiment to search for neutrinoless double beta decay in thin foils of Mo^{100} in collaboration with experimenters from Lawrence Berkeley Laboratory. Development work on the solid state silicon detectors should be complete in the next six months and construction should be well underway within the next year.

For the last several years, I have been involved in a collaborative experiment (Brookhaven AGS experiment 702) with experimenters from Yale, Brookhaven, and Pittsburgh in an attempt to measure the asymmetry parameter α in the rare, radiative decay of polarized Σ^+'s into protons and gammas. Because of inadequate kaon fluxes on the polarized target and the relatively large pion contamination in the beam in spite of several improvements to the LESB II beamline initiated by the Yale members of the collaboration, the scope of the experiment was changed to measure:

1. The Σ^+ 0 degree differential cross section in the reaction $K^-p \rightarrow \Sigma^+\pi^-$ at several incident K^- incident momenta between 600 and 800 MeV/c,
2. The sign of the asymmetry parameter α in the decay of polarized Σ^+'s into protons and neutral pions, and
3. The asymmetry parameter α in the decay of polarized Σ^-'s into neutrons and negative pions.

The final data run on this experiment was scheduled for January 1983 and actually took place during February and March. Because of a previous commitment to work full time on the development of a neutrinoless double beta decay experiment at the Lawrence Berkeley Laboratory, I was present at Brookhaven only during the February running. Although the AGS ran very poorly during this time due to H^- injection problems, and the experiment was shorthanded because Mike Zeller was immobilized in New Haven with back problems, Yale graduate student Rick Morrison and I made a number of modifications to the system electronics which resulted in a greater system reliability and stability during data taking. Cooling problems with the superconducting, polarized target magnet forced us to spend most of the February running time collecting data on the $K^-p \rightarrow \Sigma^+\pi^-$ differential cross

section rather than on the Σ decay asymmetry parameters.

Final data analysis on the February-March 1983 data, as well as the earlier May-June 1982 data is currently being carried out at Yale. A description of the superconducting magnet controller, designed and built at Mount Holyoke and used during the last two data runs, will be submitted for publication during the coming year. (It was not submitted last fall because of the opportunity to test it further in the 1983 runs.)

The majority of my research effort since August, 1982 has been on the design and development of a segmented, solid state detector array to look for neutrinoless double beta decay in Mo^{100} (See Appendix A). In August 1982, when I spent two weeks at the Lawrence Berkeley Laboratory (LBL), I wrote a Monte Carlo program which follows the path of electrons in various materials under consideration for use in the detector array. This program was subsequently extensively modified and improved by Joe Krivicich, a Berkeley graduate student at LBL and Mark Peterson, a new faculty member at Mount Holyoke (Appendix B), and a variety of possible experimental configurations were studied in detail by Joe and another Berkeley graduate student at LBL, Brian Dougherty.

Our initial design, consisting of a large number of 3mm thick germanium detector sandwiches with 20 micron Mo^{100} foil between detector pairs, was found in late January to give unacceptably broad energy resolution for the two electrons emitted in neutrinoless double beta decay. After much computer simulation of other possible designs, we finally settled in late March on a design consisting of stacks of 1.5 mm thick double sided silicon wafer detectors with about 7 micron thick disks of Mo^{100} foil between detector pairs (See Appendix A, p. 9). This design was selected for the following reasons:

1. Silicon has a lower cross section for gamma interactions than does germanium because of its lower atomic number Z. Consequently, it will have less gamma induced background.

2. Silicon has a lower probability for backscattering an incident electron than does germanium and hence electrons from Mo^{100} would be less likely to lose energy in the source material and broaden the energy resolution.

3. High purity silicon detectors can be fabricated using an oxide passivated, diffused or ion-implanted junction process which produces rugged, stable detectors with thin ($\lesssim$ 1 micron) dead layers on each side. Thus, either side of these detectors can be used next to the Mo^{100} foil, and only half as much silicon is required for the entire array.

4. Large quantities of high purity silicon are just becoming available from Komatsu (Japan) and Hughes Aircraft. Three inch high purity wafers in reasonable quantities are currently available from Wacker (Germany).

5. Lawrence Berkeley Laboratory has considerable expertise, in the person of Jack Walton and his associates, in the fabrication of high purity silicon detectors using the oxide passivation process.

I have resided in Berkeley and have been working at LBL on all aspects of the detector development work from March through August. In addition, Matthew Deady was at LBL from early June through the middle of July, working primarily on background studies by means of computer simulations and actual counting of materials at the LBL low level counting facility. During that time we and our collaborators have accomplished the following things:

i. We have done extensive computer simulations of the detector design on both real events and backgrounds.

ii. We have obtained approval from LBL to fabricate 10 grams of Mo^{100} into a 7 micron thick foil at Oak Ridge to evaluate the fabrication process for possible radioactive contamination of the Mo^{100}. (The Mo^{100} has already been extensively tested for radioactive contamination by Al Smith at the LBL low level counting facility.) The actual fabrication process will be observed at Oak Ridge by Matthew Deady to insure that no obvious sources of contamination are introduced.

iii. We have purchased from Amptek, Inc. 3 A225 hybrid chips each of which provides all of the low noise electronics necessary for a single silicon detector in the array, and have studied the performance of these chips on electronically generated pulses and on actual detectors. These chips perform satisfactorily relative to our requirements in their present form, but Amptek has also indicated a willingness to optimize the chips further for our particular application. We have also looked at TPC electronics and some low noise chips manufactured by LeCroy, but the Amptek chip appears at present to be best suited for our particular requirements.

iv. We have done extensive testing of the properties of several small silicon detectors obtained from Jack Walton. In particular, we have studied detector resolution, noise, reverse current, and breakdown voltage as a function of temperature from -150 to 25°C in a test cryostat of our own design. These tests have indicated that the demands of our large detector array can be easily met by detectors of poor quality by operating the array at reduced temperatures.

v. We have begun testing the properties of detectors fabricated from 40 mm diameter wafers of high purity Komatsu silicon. We have ordered 75-80 mm wafers of high purity Wacker silicon and expect shortly to begin

experimenting with it.

vi. We have developed an experimental facility to measure the density of surface states in oxide passivated silicon to evaluate the fabrication process on large area, high purity silicon detectors.

Because large quantities of high purity silicon is just becoming available, some development work in the fabrication of large area, high purity silicon detectors will be required. Nevertheless, very good detectors have already been made with high purity silicon using the oxide passivated, diffused junction and/or ion-implanted process, and Jack Walton foresees no fundamental problems with this technology.

Search for Lepton Violation and Massive Majorana Neutrinos: Neutrinoless Double Beta Decay of ^{100}Mo and ^{130}Te

Lawrence Berkeley Laboratory

B. Dougherty

M. Alston-Garnjost

B. Dougherty

R.W. Kenney

J.M. Krivicich

R.A. Muller

R.D. Tripp

Mt. Holyoke College

M. Deady

H.W. Nicholson

March 31, 1983

The search for neutrinoless double beta decay which has been going on for more than 30 years has acquired new interest with the advent of grand unified models favoring the abandonment of baryon and lepton number conservation and of massless neutrinos. Neutrinoless double beta decay is a sensitive indicator of the nature of the neutrino. We do not know whether the electron neutrino carries a lepton number (and is a "Dirac" particle) or if it is its own antiparticle (a "Majorana" neutrino). If the electron neutrino is a Majorana particle, and there is some current speculation among theorists that this is more natural than the Dirac alternative[1], then a search for neutrinoless double beta decay is perhaps the most sensitive way to look for neutrino mass and right-handed currents. Right-handed currents, suppressed by the heavy mass of a right-handed intermediate vector boson, would make nature right-left symmetric at very high energies.

There are two possible modes of double beta decay for a nucleus with Z protons and (A-Z) neutrons:

1) $(Z,A) \text{ --- } (Z + 2, A) + 2e^- + 2$ anti-neutrinos

2) $(Z,A) \text{ --- } (Z + 2, A) + 2e^-$.

These transitions occur primarily between nuclear ground states with spin zero and positive parity (0+) and for which single beta decay ($\Delta Z = +1$) of the parent nucleus is energetically forbidden. Geochemical evidence for double beta decay of ^{130}Te, ^{128}Te, and ^{82}Se has existed for some time[2]. Recently, the observation of the two neutrino decay of ^{82}Se has been reported[3]. However, this new experiment gives a half-life of $10^{(19.0 \pm 0.2)}$ which is 28 times smaller than that found by geochemical measurement, $10^{(20.42 \pm 0.14)}$. Recent theoretical calculations[4] agree with the newer result. A geochemical measurement[5] of the ratio of the half-lives of ^{128}Te and ^{130}Te was interpreted[2,6] as favoring the existence of both decay modes 1 and 2. However, a more recent measurement of this ratio[7] disagrees with the first by more than a factor of six and is compatible with the estimate for two-neutrino double beta decay alone.

Particularly important is whether reaction (2) occurs. Present experimental limits on the rate are in fact the best test of lepton conservation. Here neutrinoless double beta decay is only possible if the virtual anti-neutrino from the first electron emission is reabsorbed as a neutrino to permit the emission of the second electron (Fig. 1). This can occur only if the neutrino is its own antiparticle, namely a Majorana neutrino. In addition, reaction (2) requires neutrino spin-flip; this is possible only if the neutrino has a right-handed helicity component and/or the neutrino has non-zero mass.

One can prove the existence of neutrinoless double beta decay by observing a narrow peak in the sum of the energies of the two emitted electrons corresponding to the transition energy. The more copious two neutrino decay gives a broad spectrum below the narrow peak (Fig. 2).

The question of whether there are right-handed currents or whether the neutrino is massive can be resolved by studying the angular distribution of the neutrinoless double beta decay. For massive neutrinos the angular distribution is proportional to $1 - \cos\Theta$, while for right-handed currents it is proportional to $1 + \cos\Theta$, where Θ is the angle between the electrons. We can also look for transitions to the first excited state of the daughter nucleus ($J^P : 0^+ - 2^+$). These transitions can only be induced by right-handed currents.

The experiment we propose is designed to look for the neutrinoless double beta decay (reaction 2) of ^{100}Mo and ^{130}Te, but in principle we could also observe the less interesting two neutrino mode (reaction 1) with reduced sensitivity. If the neutrinoless decay mode exists, our detector can easily be modified to observe the angular distribution of the two electrons, i.e., whether they are preferentially emitted in the same or opposite directions.

The detector will be an array of elements containing approximately 1.7 mole of highly enriched double beta decay source material ^{100}Mo. An array of repeating elements, shown in Figure 3, consists of alternating layers of thin (6.6 μ) source foils between thin ($\sim$ 1.5mm) silicon solid state detectors of $\gtrsim$ 3in diameter. About 330 elements are required to view one mole of ^{100}Mo. An important feature of this system is its segmentation, a geometry that can be exploited to reduce background from cosmic rays and natural radioactivity. Each small area detector element will be observed continuously and local groups will be monitored for signals in the desired energy range. To reduce the complexity of the electronics, groups of elements will be multiplexed together. Low activity shielding will surround the counter array and an outer shield will further define radiation entering from external sources.

We have also considered germanium and compressed and liquid gas as the detector material. The relaxed cooling requirements of silicon vs. germanium and the possibility of fabricating thin dead layers on both sides of the silicon detector, making it double sided and reducing the amount of silicon required by a factor of 5 compared with Ge, makes high purity silicon a more attractive choice for detector material than germanium. The R&D required for a compressed or liquid gas ionization chamber makes it an unattractive competitor to the more straightforward silicon detector technology.

We have chosen molybdenum and tellurium for the source material because substantial quantities are available from Oak Ridge in a highly enriched form. They also have relatively large transition energies, which is important for two reasons. First, making the assumption that nuclear matrix elements for double beta decay emitters are the same, phase space considerations yield decay rates which are proportional to approximately the fifth power of the energy release. Thus, ^{100}Mo (E = 3.033 MeV) and ^{130}Te (E = 2.533 MeV) are expected to decay approximately seven and three times faster than ^{76}Ge (E = 2.045 MeV), a source used in previous and current experiments[8,9,10] For a lifetime of 10^{21} years, corresponding to a neutrino mass of 10ev or a W_R mass of 20Tev, one mole of source material would yield one neutrinoless decay per day. Second, naturally occurring backgrounds fall very rapidly with increasing energy. Figure 2 shows the measured background in the Mt. Blanc tunnel[8] along with surface measurements extending to higher energies[11]. A reasonable extrapolation of the Mt. Blanc tunnel measurements to the energy of ^{100}Mo would suggest a background falling with increasing energy approximately as E^{-6}. Inspection of the Table of Isotopes substantiates this rapid decrease beyond 2 MeV; there is a diminishing number of gamma lines with virtually nothing above 3 MeV except for some very weak (branching fractions approximately 10^{-4}) lines from RaC (^{214}Bi). Thus by using ^{100}Mo we anticipate a decrease in background by at least a factor of 10 compared to ^{76}Ge.

Further important suppression of background relative to a conventional ^{76}Ge detector can be realized due to the segmentation of our device. Only signals from the thin silicon crystals on opposite sides of the sample need be added to measure the total energy release. In this way we are dealing with many small individual volumes and not the summed background from the entire detector. Thus detection of pairs of gammas from cascading radioactive decays adding to 3 MeV is greatly reduced.

In summary, there are a number of advantages to our experimental approach.

1. Source materials can be chosen on the basis of their energy release and availability in highly enriched samples.

2. The source can be removed altogether to study backgrounds.
3. Source thickness can be varied to optimize event rate versus energy resolution.
4. The detector can be easily modified to measure the angular distribution of the electrons.
5. A measurement of the angular distribution of the electrons can be made.
6. Solid state detector materials are very pure, reducing natural backgrounds in the detector array, and very stable, making it possible to operate the detector, attended only intermittently in remote locations, such as a mine, where cosmic backgrounds can be reduced to very low levels.
7. Little R&D is required since we are using established technology.
8. Segmentation allows the start of the experiment and testing of the concept in a realistic situation with a modest investment.
9. There is a potentially much lower background, thereby compensating for the loss in energy resolution coming from the thickness of the source.
10. Low background and source-in/source-out measurements should allow us to measure the two neutrino decay spectrum of reaction 1.

Details of the experimental design are still being optimized, particularly with respect to rate and energy resolution. Fred Goulding, head of the Instruments Techniques Division of LBL, and Richard Pehl, who is in charge of advanced detector applications, both experts on solid state detectors, have assured us that aside from the normal engineering fabrication problems in building a large detector array, no technological breakthroughs are required to build what would be, as far as we know, a unique device. The expertise in solid state detector technology which exists at LBL makes it a particularly desirable site at which to develop a detector array of this type and size.

The ultimate sensitivity we hope to reach with a full array of detectors costing between \$300K and \$500K is a half-life of the order of 10^{23} years, a sensitivity to neutrino mass and to right-handed currents which is comparable to that given by a Germanium half-life of 10^{24} years. There is no compelling experimental reason to think that we will not observe lifetimes much shorter than this, perhaps as short as 10^{21} years. For this lifetime we would see one event per day.

References

1. R. Cahn, (private communication).
2. For references to early experiments, see D. Bryman and C. Picciotto, Rev. Mod. Phys. 50, 11 (1978).
3. M.K. Moe and D.D. Lowenthal, Phys. Rev. C 22, 2186 (1980).
4. W.C. Haxton, G.J. Stephenson, Jr., and D. Strottman, Phys. Rev. Lett. 47, 153 (1981) and Phys. Rev. D 25, 2360 (1982).
5. E.W. Henneke, O.K. Manual, and D.D. Sabu, Phys. Rev. C 11, 13787 (1975).
6. S.P. Rosen, "Neutrino 81", Proceedings of the 1981 International Conference on Neutrino Physics and Astrophysics, Maui 1981, 76-89 (1981).
7. T. Kirsten, Report at the workshop on "Low Energy Tests of High Energy Physics", Institute for Theoretical Physics, University of California, Santa Barbara, (1982)(unpublished).
8. E. Fiorini, A. Pullia, G. Bertolini, F. Capallani, and G. Rostelli. Nuovo Cimento 13A, 747 (1973) and E. Fiorini "Neutrino '77", Proceedings of the International Conference on Neutrino Physics and Astrophysics, Baksan Valley 1977, 2, 315 (1977).
9. F.T. Avignone III, R.L. Brodzinski, N.A. Wogman, AIP Conference Proceedings 72, 34 (1981).
10. D.O. Caldwell (private communication).
11. E. der Mateosian and M. Goldhaber, Phys. Rev. 146, 810 (1966).

Figure Captions

Figure 1 Second-order neutrinoless double beta decay.

Figure 2 The electron energy-sum spectrum from double beta decay. The neutrinoless mode is indicated by the vertical line at E_o = the nuclear transition energy. The broad spectrum, extending up to E_o, is from the two neutrino decay mode.

Figure 3 Drawings of two detector elements.

Figure 4 Measured continuum background in the Mt. Blanc tunnel[8] in 365 gm of Ge and higher energy surface measurements[11] in 20 gm of CaF_2.

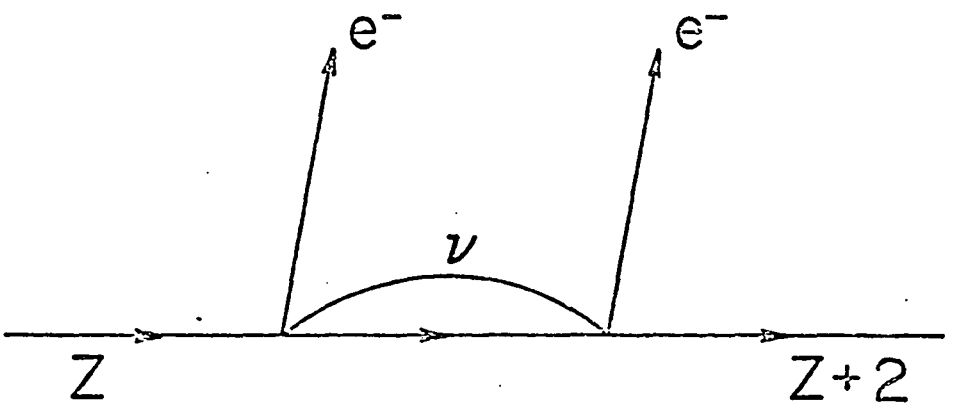

Figure 1 Second-order neutrinoless double beta decay.

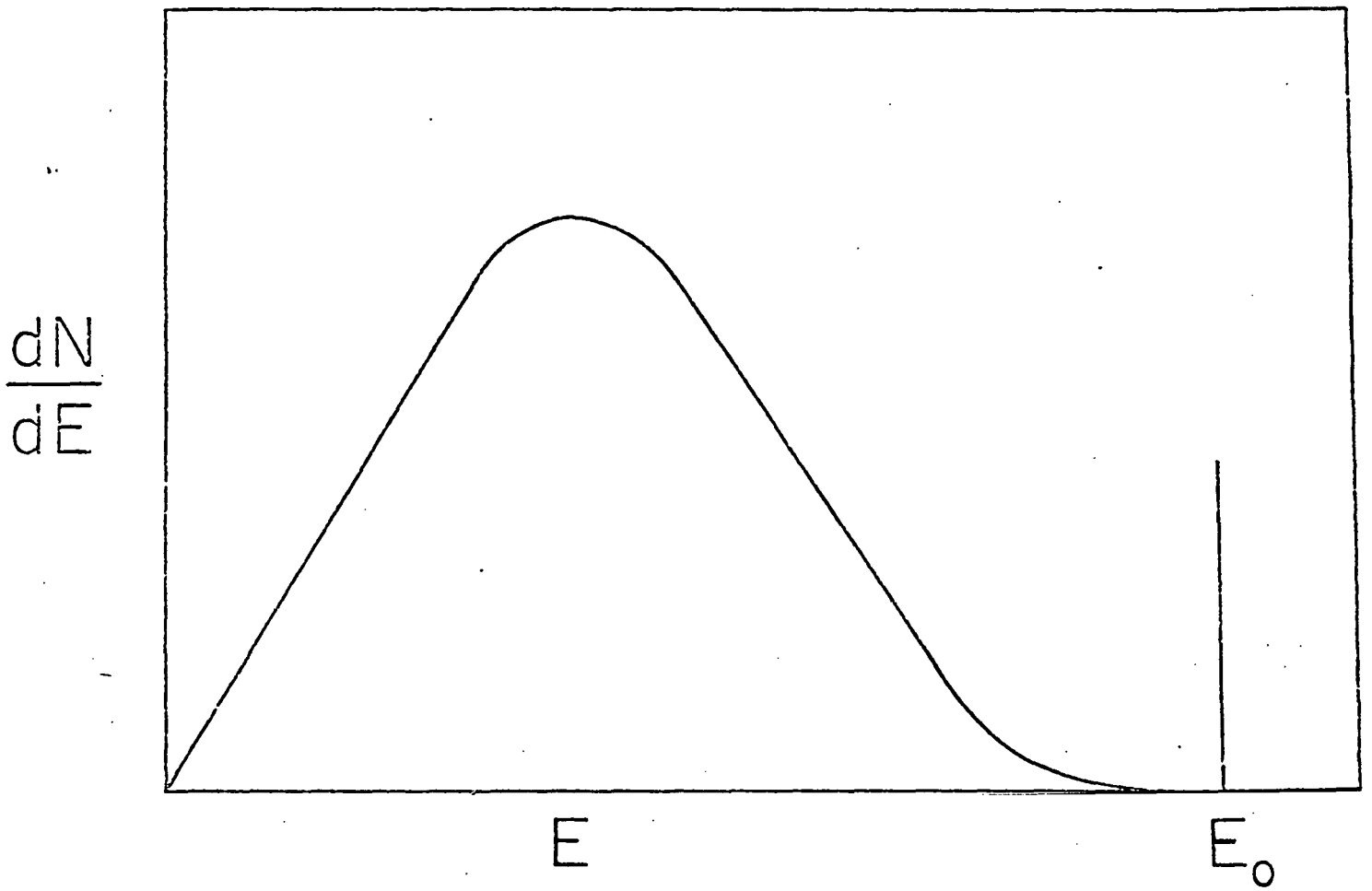

Figure 2 The electron energy-sum spectrum from double beta decay. The neutrinoless mode is indicated by the vertical line at E_o = the nuclear transition energy. The broad spectrum, extending up to E_o, is from the two neutrino decay mode.

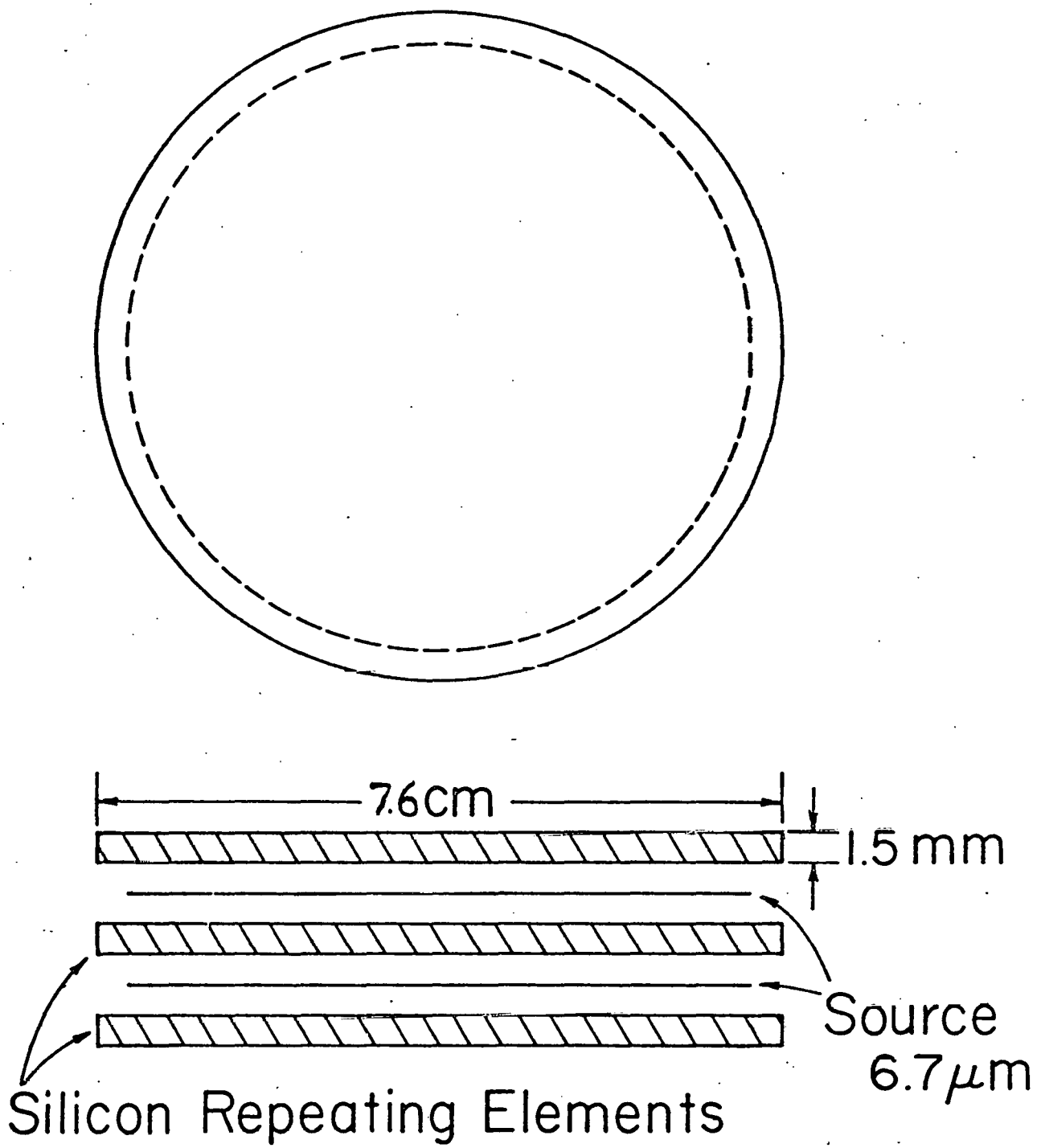

Figure 3 Drawing of two detector elements.

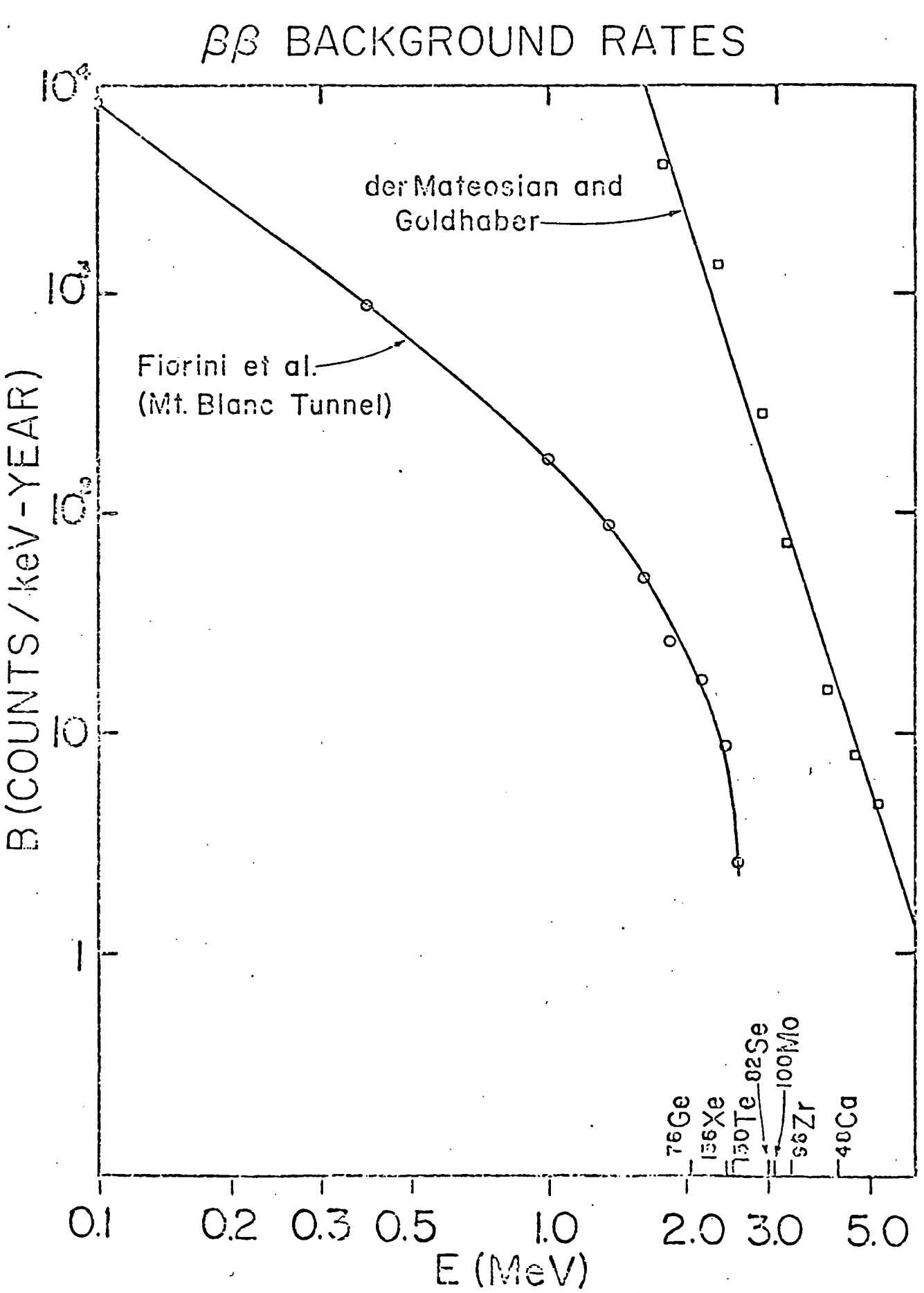

Figure 4 Measured continuum background in the Mt. Blanc tunnel[8] in 365 gm of Ge and higher energy surface measurements[11] in 20 gm of CaF.

Angular Distributions in Multiple Scattering

Mark A. Peterson

Physics Department

Mt. Holyoke College

South Hadley, MA 01075

ABSTRACT

The theory of the random walk on a sphere is derived by elementary methods and by specializing the general theory of random walks on G-spaces. The result is applied to find the angular distribution in multiple elastic scattering after N steps. The case of electron scattering from a screened Coulomb potential is done in detail. Formulae which are exact in principle and asymptotic in practice are found, giving the distribution with many-place accuracy at all angles for $N \geq 20$. Methods for generating a random variable with this distribution are also given.

Rutherford's famous analysis of α-particle scattering in gold foils distinguished two angular regimes:[1] a forward regime with a Gaussian distribution, dominated by many small-angle scatters, and a large angle regime, dominated by single scattering. This approach to the angular distribution in multiple scattering of charged particles is widely used even at the present day. It is described in textbooks.[2] It is difficult to avoid the impression that it is essentially correct.

Despite its intuitive plausibility, it is fair to ask how accurate this representation really is. Has it been thoroughly checked in physically interesting cases? The answer seems to be no. That check, for a realistic differential cross-section, considered at all angles, is made in this paper for the first time. Previous partial results, showing that the model of Fig. (1) is in fact not quantitatively accurate, are confirmed, and the comparison is extended to the entire angular range.

The method employed is not entirely new. It was given in 1940 by Goudsmit and Saunderson (GS),[3] who were, however, unable to evaluate certain coefficients in their formulae (the λ_ℓ's of Eq. (7)). Their results are rederived here in a more physical and transparent manner in Section 2, and the calculation is completed in Section 3. The result is that the usual model (Fig. 1) is significantly in error (see Fig. 2): a naive application of the central limit theorem to the forward distribution is typically about 40% low in the forward direction and may be high by a factor of 2 at somewhat larger angles where one might expect it still to apply. In addition, multiple scattering corrections to the single scattering distribution are typically significant even at the largest angles.

Curiously enough, the GS paper, which contains exact results of beautiful simplicity, has been ignored in favor of approaches which make small angle approximations. If one makes too drastic approximations one finds that the forward distribution is given by the central limit theorem.[4] This is unequivocally wrong. In the late 1940's, more careful use of the small angle approximation began to reveal the true shape of the forward distribution,[5],[6] but the results were initially often described as if they approached the naive Gaussian, even when they clearly did not.[6],[7] By 1963 it was appreciated that the forward distribution is non-Gaussian,[8] but the small-angle theories which revealed this fact are complicated and approximate, and

have never fully displaced the model of Fig. 1 in actual use.

By contrast, the methods of this paper are so simple that exact angular distributions in multiple scattering can be routinely generated for use in accurate modeling of physical processes in detectors, biological materials, etc. Until now there has been no recognized good way to do this. The persistence of Rutherford's original model (Fig. 1), despite its (more or less known) shortcomings, was perhaps due to the absence of a simple, clear alternative free of dubious approximations.

In Section 4 the method of Section 2 is related to the more general problem of a random walk on a group. The difficulty of extending this method from the angular distribution to the spatial distribution of particles undergoing multiple scattering is pointed out.

Section 5 contains practical suggestions for modelling the exact distribution.

2. Random Walk on the Sphere

Consider the distribution of a particle on the sphere which makes random jumps. It is assumed that the law governing the jumps is isotropic, homogeneous, and Markovian, i.e., that there are no preferred directions or positions, and that each jump is independent of the others. (In applying this idea to multiple scattering, the direction of travel of a particle or wave will be assumed to make such a random walk. The distribution of this random direction will be found.)

Take coordinates (θ, ϕ) on the sphere in the usual way, fixed once and for all, and use unit vectors $\hat{p}$, $\hat{q}$, etc., as a shorthand for locations (θ_p, ϕ_p), (θ_q, ϕ_q), etc. At each step of the random walk one must use the conditional probability density $W_1(\hat{p}, \hat{q})$ that a particle at $\hat{q}$ moves in the next step to $\hat{p}$. Clearly W_1 is positive with

$$\int W_1(\hat{p}, \hat{q})\, d\hat{p} = 1. \tag{1}$$

Since it is assumed that the law which governs the single step depends only on the relative direction of $\hat{p}$ with respect to $\hat{q}$, and not on any third direction, one has

$$W_1(\hat{p}, \hat{q}) = f(\hat{p}\cdot\hat{q}). \tag{2}$$

The Markovian assumption that each step is independent of the preceding one implies

$$W_N(\hat{p},\hat{q}) = \int W_1(\hat{p},\hat{R})\, W_{N-1}(\hat{R},\hat{q})\, d\hat{R} \qquad (3)$$

where $W_N(\hat{p},\hat{q})$ is the conditional probability density that a particle initially at $\hat{q}$ arrives at $\hat{p}$ after exactly N steps.

The problem posed is to find a simple expression for $W_N(\hat{p},\hat{q})$ given $W_1(\hat{p},\hat{q})$. Expand $W_1(\hat{p},\hat{q})$ in Legendre polynomials and thence in spherical harmonics:

$$W_1(\hat{p},\hat{q}) = f(\hat{p}\cdot\hat{q}) = \sum_{l=0}^{\infty} \frac{2l+1}{4\pi} \lambda_l P_l(\hat{p}\cdot\hat{q})$$

$$= \sum_{l=0}^{\infty} \sum_{m=-l}^{l} \lambda_l Y_{lm}(\hat{p})\, Y^*_{lm}(\hat{q}) \qquad (4)$$

where

$$\lambda_l = 2\pi \int_{-1}^{1} f(z)\, P_l(z)\, dz \qquad (5)$$

Then by induction in Eq. (3),

$$W_N(\hat{p},\hat{q}) = \sum_{l=0}^{\infty} \sum_{m=-l}^{l} \lambda_l^N Y_{lm}(\hat{p})\, Y^*_{lm}(\hat{q}) \qquad (6)$$

Equation (6) is the solution. In particular, taking $\hat{q}=\hat{z}$ (which only amounts to choosing the coordinate system in the most convenient way), one has

$$W_N(\hat{p},\hat{z}) = \sum_{l=0}^{\infty} \frac{2l+1}{4\pi} \lambda_l^N P_l(\cos\theta_p). \qquad (7)$$

In interpreting Eq. (7) it is useful to realize that, according to Eq. (5), the coefficient λ_l is

$$\lambda_l = \langle P_l \rangle_{W_1} \tag{8}$$

i.e., just the average value of the Legendre polynomial P_l with respect to the distribution W_1. In particular

$$\lambda_0 = 1 \tag{9}$$

and

$$|\lambda_l| < 1 \qquad \text{if } l \geq 1 \tag{10}$$

(except in uninteresting degenerate cases). Thus in the limit as $N \to \infty$, only the $l=0$ term survives in Eq. (7), and one has

$$\lim_{N\to\infty} W_N(\hat{p},\hat{q}) = \frac{1}{4\pi} \tag{11}$$

the uniform distribution on the sphere, as intuition would suggest.

If W_1 is sharply peaked forward, approximating a δ-function, $\lambda_l \doteq 1$ for a large number of terms. Finding these λ_l's accurately is the main computational difficulty in applying this method, but it is not particularly imposing. Scattering from a Thomas-Fermi atom, a problem considered by many previous investigators, yields to a simple trick (see Section 3). A cross-section parametrized by partial waves would also yield λ_l's in an obvious way.

3. Multiple Scattering from Thomas-Fermi Atoms

To apply the ideas of Section 2 to multiple scattering, note that

$$W_1 = \frac{1}{\sigma} \frac{d\sigma}{d\Omega} \tag{12}$$

i.e., W_1 is just the differential cross-section normalized to be a probability distribution. In particular, consider potential scattering of a Dirac electron from a screened Coulomb potential

$$V(r) = -\frac{Ze^2}{r} e^{-r/a} \tag{13}$$

The result, in Born approximation, is the Mott cross-section[9] modified by screening

$$W_1(x) \propto \frac{1-\beta^2 x}{(x+A)^2} \tag{14}$$

where $x=\sin^2 \theta/2$ and $A = \left(\frac{\alpha Z^{1/3}}{2\beta\gamma}\right)^2$, (15)

the latter quantity corresponding to the screening length

$$a = \frac{e^2}{\alpha^2 mc^2} Z^{-1/3} \tag{16}$$

suggested by Thomas-Fermi theory[10] (here α is the fine structure constant, β and γ are the relativistic parameters of the electron, and Z is the atomic number of the target nucleus).

The average value of the Legendre function P_l, called λ_l in Eq. (7), can be found by a generating function technique. The generating function for the average Legendre functions is just the average of their generating function, by linearity:

$$\left\langle [(1-h)^2 + 4xh]^{-1/2} \right\rangle_{W_1} = \sum_{n=0}^{\infty} h^n \lambda_n \qquad (17)$$

Define quantities $k_n(A)$ and $s_n(A)$ by

$$\int_0^1 [(1-h)^2 + 4xh]^{-1/2} (x+A)^{-1} \, dx = \sum_{n=0}^{\infty} h^n k_n \qquad (18)$$

$$\int_0^1 \left[1 + \frac{4xh}{(1-h)^2}\right]^{-1/2} (x+A)^{-1} \, dx = \sum_{n=0}^{\infty} h^n s_n = F(h) \qquad (19)$$

It is easy to see that

$$k_n = \sum_{m=0}^{n} s_m \qquad (20)$$

$$\lambda_n = \left[\beta^2 k_n + (1+\beta^2 A) \frac{dk_n}{dA}\right] / \left[\beta^2 k_o + (1+\beta^2 A) \frac{dk_o}{dA}\right] \qquad (21)$$

so that it is enough to find the s_n. Expand the first factor of the integrand in Eq. (19) by the binomial theorem and integrate. One has

$$F(h) = \sum_{n=0} \binom{-1/2}{n} z^n \left[(-A)^n \log(1+1/A) + \sum_{m=0}^{n-1} \frac{(-A)^m}{n-m}\right] \qquad (22)$$

where $z(h) = 4h/(1-h)^2$.

Now collect like powers of A:

$$F(h) = \sum_{m=0}^{\infty} (-A)^m \left[\binom{-1/2}{m} z^m \log(1+1/A) + F_m(h) \right] \qquad (23)$$

where

$$F_m(h) = z^m \lim_{\epsilon \to 0} \int_{\epsilon}^{\infty} [(1+\zeta)^{-1/2}]_m \, \zeta^{-m-1} \, d\zeta \qquad (24)$$

and $[\ ]_m$ means the first m terms of the Maclaurin expansion are subtracted off.

It is now straightforward, though tedious, to find F(h) as a power series in h (and hence to find s_n) through any finite power of A in the expansion of Eq. (23). The result for s_n through terms involving A^3 is

$$s_n = a_n \log(1+1/A) + b_n + c_n A\log(1+1/A) + d_n A + e_n A^2\log(1+1/A) + f_n A^2 + g_n A^3\log(1+1/A) + h_n A^3 + \mathcal{O}(n^7A^4\log A) \qquad (25)$$

where

$$\begin{aligned}
a_n &= \delta_{no} \\
b_n &= [-2/n]\, \epsilon_{n1} \\
c_n &= 2n\, \epsilon_{n1} \\
d_n &= -[\,2(n-1) + 4n\,(1/2 + 1/3 + \ldots + 1/n)\,]\, \epsilon_{n2} \\
e_n &= (n+1)n(n-1)\, \epsilon_{n2} \\
f_n &= -[\,4n(n-1)(n-2)/3 - (n-1)(n-2)(n-3)/6 \\
&\qquad +2(n+1)n(n-1)(\,1/4 + 1/5 + \ldots + 1/(n+1))]\, \epsilon_{n3} \\
g_n &= [(n+2)(n+1)n(n-1)(n-2)/6]\, \epsilon_{n3}
\end{aligned} \qquad (26)$$

$$h_n = -\left[\frac{1}{4}(n+1)n(n-1)(n-2)(n-3) - \frac{1}{20} n(n-1)(n-2)(n-3)(n-4) \right.$$

$$+\frac{1}{180}(n-1)(n-2)(n-3)(n-4)(n-5)$$

$$\left. + \frac{1}{3}(n+2)(n+1)n(n-1)(n-2)\left(\frac{1}{6} + \frac{1}{7} + \ldots + \frac{1}{n+2} \right) \right] \theta_{n4}$$

$$\delta_{nm} = \begin{cases} 1 \text{ if } n=m \\ 0 \text{ if } n \neq m \end{cases}$$

$$\epsilon_{nm} = \begin{cases} 1 \text{ if } n \geq m \\ 0 \text{ if } n < m \end{cases}$$

A similar expression for λ_n follows from Eqs. (20) and (21). Using this expression for λ_n in Eq. (7) gives a formula for W_N which for many purposes is essentially exact, a remark we now justify.

The series obtained for λ_n from Eqs. (23), (15), (20) and (21) converges (in fact it is exact after 2n+1 terms). More important for practical purposes, only the first few terms, typically just those given in Eq. (25), are necessary in applications, by the following argument.

The terms in Eq. (25) decrease rapidly if $n \ll A^{-1/2}$, so that one may expect Eq. (25) to be accurate up to some n_{max} which depends on A. An estimate of n_{max} is given by looking at the next term in the expansion for s_n in Eq. (25), namely

$$s_n = \ldots + j_n A^4 \log(1+1/A) \qquad (27)$$

where $j_n = (n+3)(n+2)(n+1)n(n-1)(n-2)(n-3)/72$

Requiring this term to be less than, say, .001 gives

$$n_{max} \doteq [.072\ A^{-4}/\log(1+1/A)]^{1/7} \tag{28}$$

Now take N, the number of steps, to be so large that the contribution of the term containing $\lambda_{n_{max}}^{N}$ is negligible, even at $\theta = \pi$, where the cancellation of terms is especially delicate. Using the estimate $W_N(\pi) = NW_1(\pi)$ and asking for 3-figure accuracy there, one finds

$$N \gtrsim \log\left(\frac{4\pi W_1 \times 10^{-3}}{2n_{max}+1}\right) \Big/ \log(\lambda_{n_{max}}) . \tag{29}$$

So long as N satisfies this inequality (which is quite insensitive to the detailed assumptions in its derivation), W_N is accurate at all angles. In fact, the inequality turns out to be

$$N \gtrsim 20 \tag{30}$$

showing little explicit dependence on electron energy up to 3 Mev, which covers the range of most natural β emitters. Of course, for higher energy W_1 is sharper (A is smaller) so that more terms in Eq. (7) are needed to represent W_N. But just because A is smaller, the expansion of Eq. (25) does provide those terms. (W_{20} for a 3 Mev electron in germanium requires nearly 500 terms. For larger N, far fewer are needed.)

The procedure outlined above could be extended to $N < 20$ by going farther in the expansion of Eq. (25). For example, with the next term (Eq. (27)) included, W_{15} appears to be accurate.

The above discussion does not give rigorous estimates of error, but experience has shown it to be an accurate rule of thumb. The formula for W_N is asymptotic in N. The error in W_N appears to be $\mathcal{O}(\epsilon^N)$ where $\epsilon^{20} \leq .02 W_1(\pi) << 1$.

A typical result for W_N is shown in Fig. 2, with the Gaussian distribution of the central limit theorem and the single scattering tail NW_1 for comparison. The results of work using small angle approximations is confirmed in the forward direction, and comparisons at large angles are possible for the first time. Multiple scattering corrections to the single scattering distribution are quite noticeable.

In summary, Eq. (7) with λ_1 given by Eqs. (20), (21), and (25) is an explicit solution to the multiple scattering problem for $N \gtrsim 20$ with many-place accuracy at all angles.

4. Random Walks on Groups

One gets a deeper insight into the formulae of Section 2 by considering them in a more general setting, that of a random walk on a group.[11] In particular one sees that the reason the forward distribution in multiple scattering is non-Gaussian is that it arises as a random walk in a non-Euclidean space, whereas the central limit theorem is associated in an essential way with random walks in Euclidean spaces and more particularly with the Euclidean translation group.

A random walk on a group G can be identified with a random sequence of group operations in which G operates on itself by left multiplication. The group operations have a linear representation ρ on the space $\mathcal{F}$ of real valued functions on the group in the usual way[13]

$$\rho(g)\ f(h) = f(hg^{-1}) \tag{31}$$

In what follows, the notation will imply that G is a finite group, but nothing is changed if G is a compact Lie group and summation over G is interpreted as integration with respect to Haar measure.[13]

Let p_1 be a probability measure on G such that $p_1(g)$ is the probability of a translation in a single step by the action of g on G. (We assume that the random walk can be characterized in this way, i.e., that the probability

of the step h $\longrightarrow$ gh is independent of h.) Similarly, let $p_N(g)$ be the probability that in N steps one has translated by the action of g. Then

$$p_N(g) = \sum_{h \in G} p_1(gh^{-1}) p_{N-1}(h) \tag{32}$$

Define an operator $\hat{A}$ on functions using the representation ρ[12]

$$W[p_1] = \sum_{g \in G} p_1(g) \rho(g) \tag{33}$$

Then it is easy to prove by induction that

$$(W[p_1])^N = W[p_N] . \tag{34}$$

For suppose $(W[p_1])^N = \sum_{h \in G} p_N(h) \rho(h)$. Then

$$\begin{aligned}
(W[p_1])^{N+1} &= \sum_{g \in G} \sum_{h \in G} p_1(g) \rho(g) p_N(h) \rho(h) \\
&= \sum_{g \in G} \sum_{h \in G} p_1(g) p_N(h) \rho(gh) \qquad (35) \\
&= \sum_{j \in G} \sum_{h \in G} p_1(jh^{-1}) p_N(h) \rho(j) \\
&= \sum_{j \in G} p_{N+1}(j) \rho(j) = W[p_{N+1}]
\end{aligned}$$

$W[p_1]$ is essentially the stochastic matrix for the random walk.

An important simplification occurs if $p_1(g)$ is a class function, i.e., if

$$p_1(g) = p_1(hgh^{-1}) \qquad \forall\, h \in G \tag{36}$$

In this case, $W[p_1]$ can be written as

$$W[p_1] = \sum_{[k]} p(k) \sum_{h \in C_k} \rho\ (h) \tag{37}$$

where $k \in C_k$ is any representative from the class C_k of G. The operator

$$\langle \rho \rangle_k \overset{\text{def}}{=} \sum_{h \in C_k} \rho\,(h) \tag{38}$$

is a scalar multiple of

$$\langle\langle \rho \rangle\rangle_k \overset{\text{def}}{=} \sum_{g \in G} \rho\,(gkg^{-1}) \tag{39}$$

However,

$$\begin{aligned} \langle\langle \rho \rangle\rangle_k\, \rho\,(h) &= \sum_{g \in G} \rho\,(gkg^{-1})\, \rho\,(h) \\ &= \sum_{g \in G} \rho\,(gkg^{-1}h) \\ &= \sum_{j \in G} \rho\,(hjkj^{-1}) \\ &= \sum_{j \in G} \rho\,(h)\ \rho\,(jkj^{-1}) \\ &= \rho\,(h) \langle\langle \rho \rangle\rangle_k \end{aligned} \tag{40}$$

Thus, by Schur's lemma, $\langle\langle \rho \rangle\rangle_k$ is just a multiple of the identity operator I on each irreducible representation contained in ρ . If we take as a basis in $\mathcal{F}$ a basis for the irreducible representations contained in ρ , then $W[p_1]$ is diagonal, so that raising it to the Nth power (i.e., computing the effect of a random walk of N steps) is trivial.

A space M on which G acts transitively can be identified with G/H, where H is the isotropy group of a point of M.[14] If H is a symmetry of p_1, the random walk analysis on G passes to the quotient M. Thus the random walk on the sphere can be regarded as arising from a random walk on SO(3) with p_1 a class function. It passes to the quotient SO(3)/SO(2), which is just the 2-sphere. Eq.(6) displays W_1 in diagonal form, as it was guaranteed to be, because the spherical harmonics are a basis for the irreducible representations of SO(3) on S^2. (The spherical harmonics themselves arise by the quotient procedure: they are just the symmetric top wave functions which are invariant under the action of the SO(2) in the quotient.)

It is disappointing that the same observation cannot be used to solve the multiple scattering problem in its entirety, i.e., to find the spatial distribution of particles together with their angular distribution. This amounts to solving the random walk on the affine group of translations

and rotations in 3-space. Curiously enough, the probability measure that corresponds to physical scattering processes is not a class function on this group. Thus the stochastic matrix W_1 cannot be diagonalized using group theory alone: the correct basis functions depend on the details of p_1 and cannot be found once and for all, as in the simpler angular problem.

5. Modelling with W_N

In modelling multiple scattering one wishes to generate a random variable Θ with the distribution W_N. This is not immediately easy, even though W_N is a known function.[15],[16]

Call f a rapidly-generable (RG) function on a domain D if it is a probability distribution, i.e. $f \geq 0$ on D,

$$\int_D f = 1 \tag{41}$$

and if there is a rapid procedure for generating a random variable with distribution f. (This definition is flexible: what it means depends on context, but it seems to be a useful notion.)

To be concrete, let D be the interval [0,1]. Then by most standards the uniform distribution f=1 is RG. Also, if for any probability distribution f we define

$$g(x) \overset{\text{def}}{=} \int_0^x f(x')dx' , \tag{42}$$

then the random variable $x=g^{-1}(y)$, where y is uniformly distributed on [0,1], has distribution f. Thus f is RG if g^{-1} is rapidly computable.

If $f_1,\ldots,f_n$ are RG, and nonnegative numbers $a_1,\ldots,a_n$ satisfy $a_1+\ldots+a_n = 1$, then $f = a_1f_1+\ldots+a_nf_n$ is RG, that is, appropriate linear combinations of RG functions are RG.

In this language, the problem is to approximate W_N by an RG function. In general, it is not clear that a solution exists at all, since the RG functions may not be dense in the space of the W_N's in the appropriate norm.

The following observations constitute a rough-and-ready solution to the problem of finding an RG approximation to W_H on the sphere. This is not a solution in the sense of giving an RG sequence $\{f_n\}$ which converges to W_N. Rather we find functions which are within a few percent at all angles.

Define a family of functions

$$F(\alpha;x) = \frac{e^{-4\alpha x}}{1-e^{-4\alpha}} \quad \frac{\alpha}{\pi} \tag{43}$$

For any α, F is a probability distribution in x on [0,1] with respect to the measure $4\pi\,dx$, and it is RG. (We are really thinking of $x=\sin^2\theta/2$ and F as a distribution on the sphere. The form is chosen so that F looks as nearly as possible like a Gaussian in θ with width α^{-1}.) It turns out that linear combinations of such functions can approximate W_N well in the forward direction.

For large angles ($x \geq x_T \simeq \sin^2\theta_{rms}$) the form

$$G(A,B,C,x_T;x) = \frac{B+Cx}{(A+x)^2}\ \theta(x-x_T), \tag{44}$$

suggested by the single-scattering distribution, works well.

In order that the two forms join well at x_T, it is advantageous to define "folded F's" on $[0,x_T]$:

$$\hat{F}(\alpha,x_T;x) = [F(\alpha;x) + (1-x_T)\,F(\alpha,x')/x_T]\,\theta(x_T-x) \qquad (45)$$

where $x'(x) = 1 - x\,(x_T^{-1} - 1)$.

$\hat{F}$ is RG because it corresponds to the following procedure: 1) generate a variable ξ' with distribution F, 2) if $\xi' \le x_T$ set $\xi = \xi'$, 3) if $\xi' > x_T$, set $\xi = x_T(1-\xi')/(1-x_T)$.

ξ is a random variable with distribution $\hat{F}$.

The function $G(A,B,C,x_T;x)$ is RG because if y is uniformly distributed on $[0,1]$, the iterative procedure

$$x_0 = x_T$$

$$x_n = \xi_1 + (A+x_{n-1})(A+x_T)C\,\log\left(\frac{A+x_{n-1}}{A+x_T}\right)/\xi_2 \qquad (46)$$

where $\xi_2 = y(A+x_T)-(B-AC)$

$$\xi_1 = [(AG-B)x_T - yA(A+x_T)]\,/\xi_2$$

converges to a random variable x whose distribution is G.

It is straightforward to find positive constants $a_1, a_2, \ldots, a_{n+1}$, and $\alpha_1, \ldots, \alpha_n$ such that $a_1+\ldots+a_{n+1} = 1$ and

$$W_N \doteq a_1\hat{F}_1+\ldots+a_n\hat{F}_n + a_{n+1}G. \qquad (47)$$

It does not seem to be possible to use the same form for all parameter values, however. Modelling electrons in germanium, with $100 \le N \le 200$ required the rather inelegant choices of Table 1 at various energies.

A typical W_N, with its RG approximant (nearly indistinguishable from it) is shown in Fig. 3.

In summary, the observations of this section facilitate fast, accurate modelling of angular distributions in multiple scattering.

The work was supported by the High Energy Physics Division of the U.S. Department of Energy under contract no. ER-78-5-02-4831.

ACKNOWLEDGEMENT

Thanks to Howard Nicholson, Jr., for directing my attention to this problem.

Electron energy	Distribution
$E \leq 0.52$ Mev	uniform
$0.52 < E \leq 0.6$ Mev	$F(\alpha)$
$0.6 < E \leq 0.9$ Mev	$a\hat{F}(\alpha) + (1-a)G$
$0.9 < E \leq 4.5$ Mev	$a_1\hat{F}(\alpha_1) + a_2\hat{F}(\alpha_2) + a_3G$

Table 1. Form of the RG distribution approximating W_N in germanium for $100 \leq N \leq 200$. The functional forms F, $\hat{F}$, and G are defined in the text.

FIGURE CAPTIONS

Fig. 1. The Rutherford model for the angular distribution in multiple scattering, showing two angular regimes, with a Gaussian distribution forward and single scattering backward. The crossover region, where some kind of interpolation appears to be called for, is sometimes called "plural scattering."

Fig. 2. Comparison of the Rutherford model with the exact angular distribution, found as described in the text, for a 1.9 Mev electron in germanium after 150 scatters. There is a significant discrepancy, of the order of 10%-50%, at almost all angles.

Fig. 3. The exact distribution of Fig. 2 is well approximated by the form given in Table 1 with parameters $a_1=0.572$, $a_2=0.393$, $a_3=0.034$, $\alpha_1=18.1$, $\alpha_2=40.0$, $A=-0.0190$, $B=0.00381$, $C=-0.00349$, $x_T=0.00586$.

REFERENCES

1. Rutherford, E., Phil. Mag. 21 (1911), 669.

2. Jackson, W.D., Classical Electrodynamics, 2nd ed., John Wiley and Sons, 1975, p. 647 ff.

3. S. Goudsmit and J.L. Saunderson, Phys. Rev. 57 (1940), 24.

4. E. Fermi, as quoted in B. Rossi and K. Greisen, Rev. Mod. Phys. 13, (1941), p. 265 ff.

5. Molière, G., Z. Naturforsch., 3a, (1948),78.

6. Snyder, H.S. and Scott, W.T., Phys. Rev. 76, (1949), 220.

7. Rossi, B., High-Energy Particles, Prentice Hall, Inc., NY, 1952, p. 75.

8. Scott, W.T., Rev. Mod. Phys. 35 (1963), 231.

9. Bjorken, J.D. and Drell, S.D., Relativistic Quantum Mechanics, McGraw-Hill, Inc., NY, 1964, p. 106.

10. Schiff, L.I., Quantum Mechanics, McGraw-Hill, Inc., NY, 1955.

11. Wigner, E.R., Phys. Rev. 94 (1954), 17.

12. This transform of p_i, analogous to the Fourier transform, is introduced by Persi Diaconis in Group Theory in Statistics, (unpublished) notes for a course taught at Harvard, Spring, 1982.

13. Mackey, G.W., Induced Representations of Groups and Quantum Mechanics, W.A. Benjamin, Inc., 1968.

14. Zelobenko, D.P., Compact Lie Groups and their Representations, American Mathematical Society, Providence, R.I., 1973, p. 377 ff.

15. Rubinstein, R.Y., Simulation and the Monte Carlo Method, Chapter 3, John Wiley and Sons, NY, 1981.

16. Chambers, J.M., Computational Methods for Data Analysis, Chapter 7, John Wiley and Sons, NY, 1977.

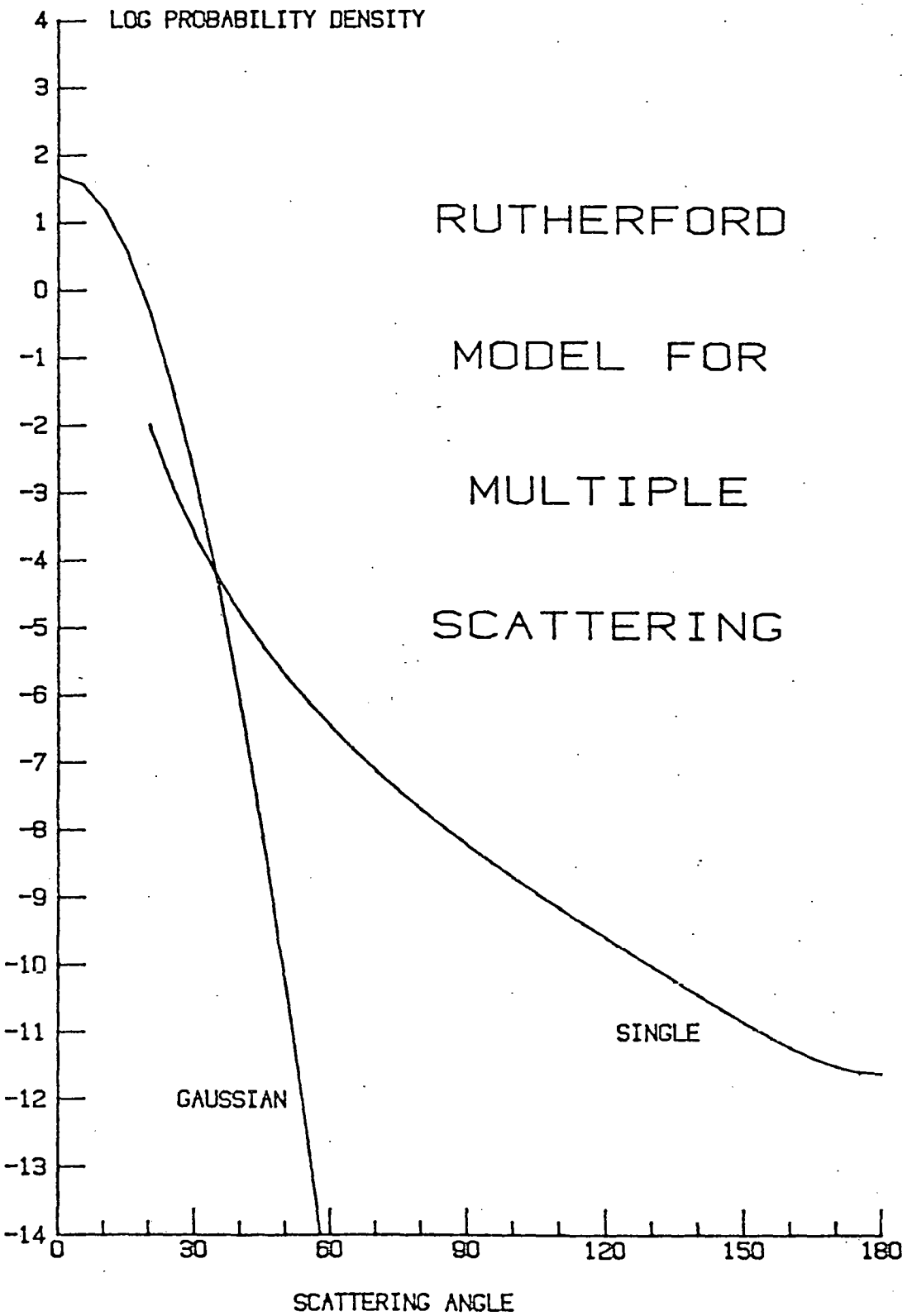
LOG PROBABILITY DENSITY
4
3
2
1
0
-1
-2
-3
-4
-5
-6
-7
-8
-9
-10
-11
-12
-13
-14
0
30
60
90
120
150
180
SCATTERING ANGLE
RUTHERFORD
MODEL FOR
MULTIPLE
SCATTERING
SINGLE
GAUSSIAN

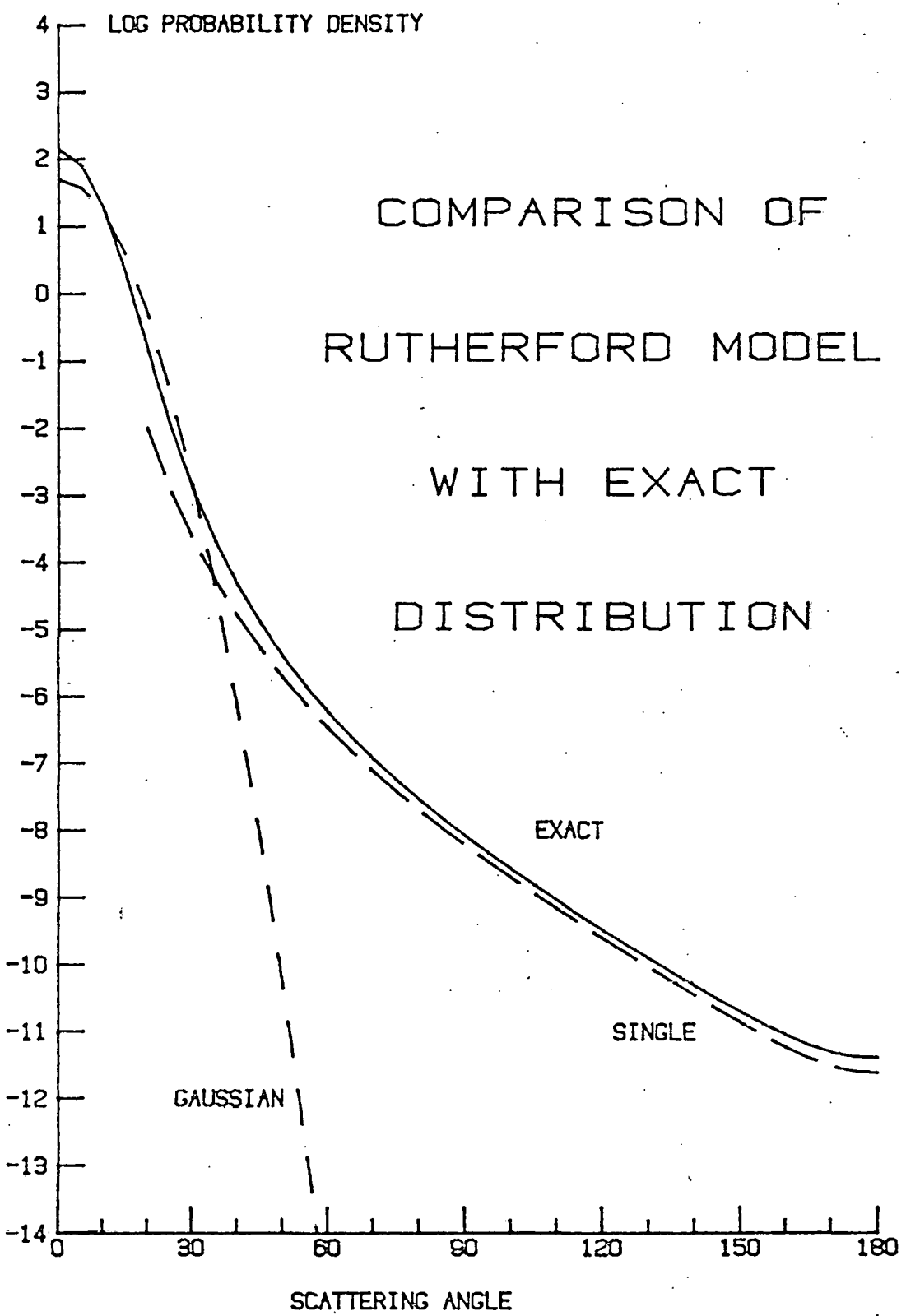
LOG PROBABILITY DENSITY
4
3
2
1
0
-1
-2
-3
-4
-5
-6
-7
-8
-9
-10
-11
-12
-13
-14
0
30
60
90
120
150
180
SCATTERING ANGLE
COMPARISON OF
RUTHERFORD MODEL
WITH EXACT
DISTRIBUTION
EXACT
SINGLE
GAUSSIAN

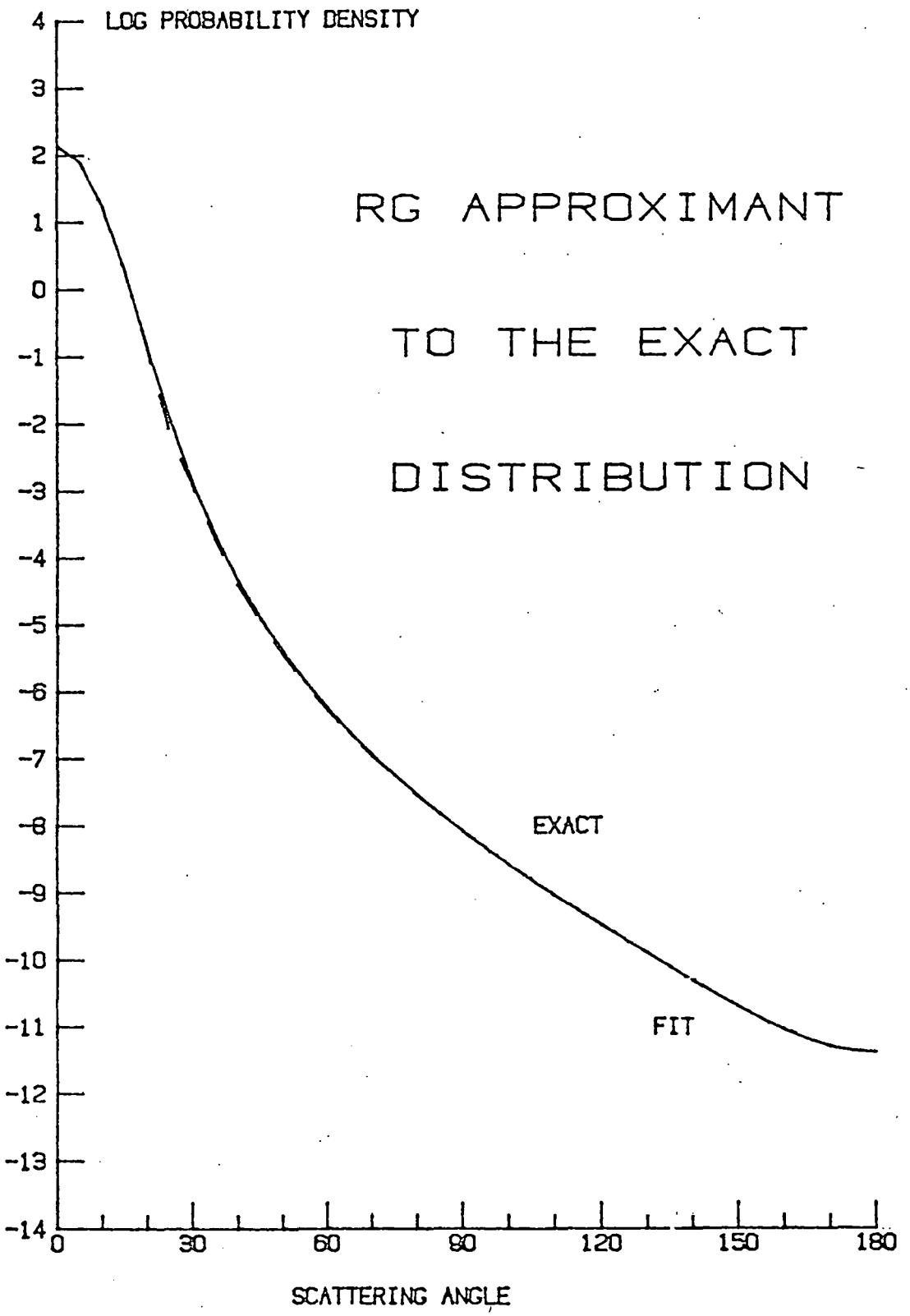
LOG PROBABILITY DENSITY
4
3
2
1
0
-1
-2
-3
-4
-5
-6
-7
-8
-9
-10
-11
-12
-13
-14
0
30
60
90
120
150
180
SCATTERING ANGLE
RG APPROXIMANT
TO THE EXACT
DISTRIBUTION
EXACT
FIT